Ann. Geophys., 29, 1355–1363, 2011
www.ann-geophys.net/29/1355/2011/
doi:10.5194/angeo-29-1355-2011

Annales Geophysicae

Observations of AGW/TID propagation across the polar cap: a case study

H. T. Cai[1,2], **F. Yin**[1,2], **S. Y. Ma**[1,2], **and I. W. McCrea**[3]

[1]Department of Space Physics, School of Electronic Information, Wuhan University, 430079, China
[2]Key Laboratory of Geospace Environment and Geodesy, Ministry of Education of PRC, Wuhan, 430079, China
[3]Space Science and Technology Department, Rutherford Appleton Laboratory, Chilton, Oxfordshire, OX11 0QX, UK

Received: 6 December 2010 – Revised: 14 July 2011 – Accepted: 18 July 2011 – Published: 12 August 2011

Abstract. In this paper, we present observational evidence for the trans-polar propagation of large-scale Traveling Ionospheric Disturbances (TIDs) from their nightside source region to the dayside. On 13 February 2001, the 32 m dish of EISCAT Svalbard Radar (ESR) was directing toward the geomagnetic pole at low elevation (30°) during the interval 06:00–12:00 UT (MLT $\approx$ UT + 3 h), providing an excellent opportunity to monitor the ionosphere F-region over the polar cap. The TIDs were first detected by the ESR over the dayside north polar cap, propagating equatorward, and were subsequently seen by the mainland UHF radar at auroral latitudes around geomagnetic local noon. The propagation properties of the observed ionization waves suggest the presence of a moderately large-scale TIDs, propagating across the northern polar cap from the night-time auroral source during substorm conditions. Our results agree with the theoretical simulations by Balthazor and Moffett (1999) in which poleward-propagating large-scale traveling atmospheric disturbances were found to be self-consistently driven by enhancements in auroral heating.

Keywords. Ionosphere (Ionosphere-atmosphere interactions; Polar ionosphere; Wave propagation)

1 Introduction

The investigation of Atmospheric Gravity Waves and/or Traveling Ionospheric Disturbances (AGW/TIDs) has been the subject of continuous research interest since the paper of Hines (1960). Properties of AGW/TID have been investigated extensively by numerous authors through the past four decades, by means of observations and numerical simulation (e.g. Hocke and Schlegel, 1996 and references therein). The interpretation of TIDs as being the ionospheric manifestations of AGWs has been supported by a large number of researchers. These gravity waves are generally accepted to be generated in the auroral or sub-auroral region, as a result of Joule heating and Lorentz forces induced by auroral electrojects and particle precipitation (e.g. Hall et al., 1999; Innis and Conde, 2002). The AGWs/TIDs with horizontal scale of $\sim$1000 km are often referred as "large-scale" waves, propagating predominantly equatorward from high latitudes (Hunsucker, 1982). Large-scale AGWs/TIDs play an important role in the dynamics of the thermosphere as they propagate away from the source region, leading to global energy redistribution (Yeh and Liu, 1974).

Based on classical gravity-wave theory, Richmond (1978) claimed that a point source would result in an isotropically propagating disturbance. AGW/TID propagation equatorward of the auroral region has been measured extensively by experimental campaigns during the Worldwide Atmospheric Gravity-wave Study (e.g. Williams, 1988; Williams et al., 1993). Most recently, characteristics of large-scale TIDs during magnetic storms have been reported by a number of authors (e.g. Shiokawa et al., 2007; Ding et al., 2008; Valladares et al., 2009). However, theoretical and observational studies of AGW/TID propagation poleward of the auroral region are relatively rare, partly due to the limitations in available observations of the thermosphere and the ionosphere at extremely high latitudes. Using a fully coupled thermosphere-ionosphere-plasmasphere model, Balthazor and Moffett (1999) investigated the morphology of large-scale TIDs propagating poleward from auroral sources and claimed that poleward-propagating large-scale traveling atmospheric disturbances could be self-consistently driven by enhancements in auroral heating. The modeling results of Shiokawa et al. (2007) also imply that large-scale TIDs can

Correspondence to: H. T. Cai
(htcai@whu.edu.cn)

Published by Copernicus Publications on behalf of the European Geosciences Union.

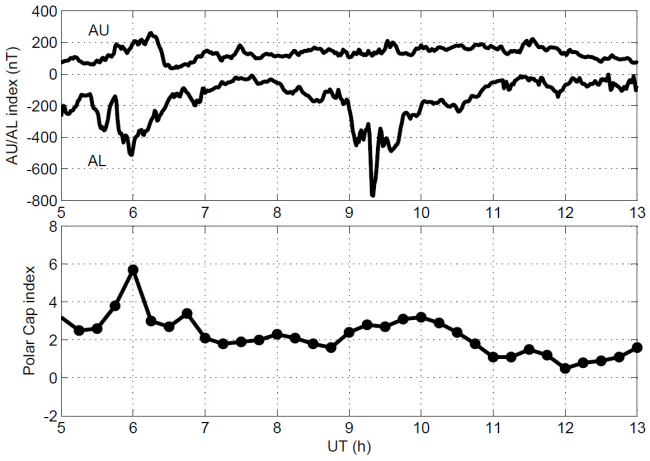

Fig. 1. AU/AL indices from WDC for Geomagnetism, Kyoto (top panel) and Polar Cap index from WDC for Geomagnetism, Copenhagen (bottom panel) in the interval of 05:00–13:00 UT on 13 February 2001.

cross the polar region. In the polar cap, distinctive signatures in the neutral atmosphere, induced by gravity waves, were reported by Johnson et al. (1995), while MacDougall et al. (1997) also described properties of polar cap gravity waves in the ionosphere F-region. Recently, observational evidence of gravity waves in the southern polar cap has been presented by Innis et al. (2001).

In this paper, we contribute further observations of poleward-propagating AGW/TID generated somewhere on the nightside during substorm conditions, which appear to have crossed the northern polar cap from the nightside and subsequently arrived at dayside auroral region. The characteristics of TIDs derived from observations of the ESR and the mainland UHF radar are summarized in Sect. 2. In Sect. 3, the properties of the polar cap AGW/TID are compared with previous results. A brief summary is presented in Sect. 4.

2 Observations

The AGW/TID event presented in this paper was observed during the period 06:00–12:00 UT on 13 February 2001. The Kp index varied between 4^+ and 3, suggesting moderate geomagnetic activity. The AU/AL and Polar Cap Indices during the time interval of interest are shown in Fig. 1. It can be noted that AL index exhibited two negative peaks around 06:00 and 09:20 UT, indicating temporal enhancements in the strength of the westward electrojet. The Polar Cap index varied somewhat during the interval, with its magnitude being generally lower than 4 except for that at 06:00 UT ($p = 5.7$).

The selected data are observations from the EISCAT Svalbard radar (ESR, 78° N, 16° E, corrected geomagnetic latitude (MLat) = 75° N) and the EISCAT UHF radar at Tromsø (69.6° N, 19.2° E, MLat = 66.7° N). The fixed 42 m dish at Svalbard and the EISCAT UHF radar at Tromsø were both measuring along the local geomagnetic field lines and the two radar sites are close to being longitudinally aligned. During the interval of 06:00–12:00 UT, the steerable 32 m dish of ESR was operating at low elevation (30°), directed toward the northern geomagnetic pole. The maximum range of the 32 m dish of ESR exceeds 1000 km, covering a rather broad horizontal range in the polar cap up to ∼80° MLat.

In order to clearly show the wave signatures measured during this interval, we have used values of ionospheric absolute disturbances, $\delta F = F - F^0$, where F represents one of the ionospheric parameters: electron density and temperature (N_e, T_e), ion temperature (T_i) and ion bulk velocity in the line of sight (V_i). The values of these disturbances have been obtained by removing the backgrounds F^0 which contain tidal and other long period variations. The backgrounds have been derived from the observed radar data by smoothing with a moving rectangular time window. Since it was suggested by Hocke (1996) that disturbances with period >2.5–3 h could be associated with tidal modes, a smoothing window width of 2.5 h has been employed in the present research. A zero-phase lowpass (Butterworth type) digital filter was applied to remove any high-frequency variations in δF. Contours of the height dependent power spectral density (PSD) of δF were carefully checked and common maximum values of the estimated PSD over a range of periods from 100 to 250 min were found for all four ionospheric parameters at altitudes above ∼250 km (not shown). In this way, the low-pass filter was designed to allow variations in δF with period longer than 100 min to pass through. Relative fluctuations, $\delta F/F^0$ (%) were calculated for each of N_e, T_e and T_i. Finally, the time-varying values of $\delta F/F^0$ (%) (or δF for V_i) at various altitudes (geomagnetic latitudes) were analyzed, and the results are reported in the following sections.

2.1 Field-aligned observations

2.1.1 ESR 42 m dish

Figure 2a shows a color-coded plot of the electron density observed by the field-aligned 42 m dish of ESR. The ESR initially moved into the cusp around 09:20 UT (∼12:20 MLT), as indicated by the temporal ionization increase accompanied by enhancements of electron temperature (not shown). The backgrounds and absolute disturbances of electron density are also displayed in panel b and c, respectively. Figure 2d summarizes the characteristics of electron density relative fluctuations derived from observations of the 42 m dish. Clear periodic signatures can be noted in the time variation of the fluctuations, having a period of around 120 min. The TID can also be identified by the inclined wavefronts of the ionization fluctuations in panels c and d, which are very similar to the characteristics of TIDs induced by upward propagating

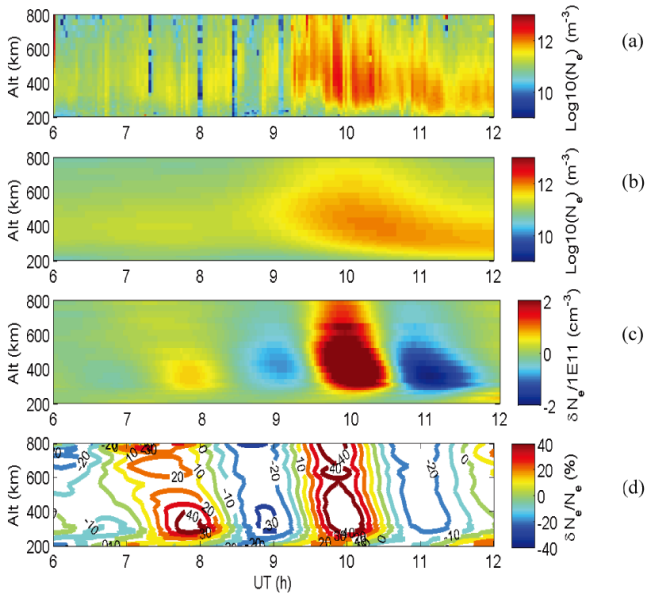

Fig. 2. From top to bottom, **(a)** overview of electron density (N_e) observed by the fixed field-aligned 42 m dish of ESR as a function of UT and altitude; **(b)** N_e background by applying a zero-phase filter with a moving window of 2.5 h; **(c)** electron density absolute disturbances, δN_e by subtracting N_e background from the observed density displayed in panel **(a)**; and **(d)** fractional electron density fluctuations, $\delta N_e/N_e$ (%) in relative to the background level displayed in panel **(b)**.

AGW with downward progressing wavefronts. According to the theory of gravity waves, the group velocity of large-scale AGWs in the ionospheric F-region usually has a slightly upward tilt, while the phase velocity has a sharply downward tilt. Thus, the phase velocity of TIDs induced by an upward propagating AGW has a downward component, leading to inclined wavefronts observed in the contours of the ionospheric fluctuations.

The physics of the gravity wave-TID relationship has been theoretically elucidated by Kirchengast (1996) and Kirchengast et al. (1996), who concluded that AGWs could be established as the cause of an observed TID by using the "polarization information" obtained along a single incoherent scatter beam. Furthermore, the characteristics of high-latitude TIDs from different causative mechanisms were numerically compared in detail by Kirchengast (1997) and the TID information derivable from ISR data was found to show features which distinguished different meachanisms sufficiently to allow their identification, especially for AGW-induced TIDs. In our case, however, geomagnetic conditions (Fig. 1) were such that the observed TID could have been biased by other ionospheric activity, such as wavelike variations in $\boldsymbol{E} \times \boldsymbol{B}$ drift strength or fluctuations in particle precipitation intensity. Hence, some additional features of the TID need to be checked to convincingly establish AGWs as the source of the observed signatures.

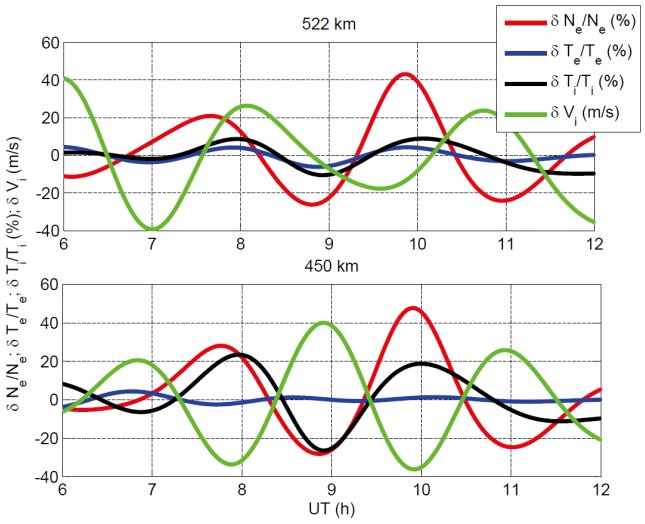

Fig. 3. Time series of the TID quantities ($\delta N_e/N_e^0, \delta T_e/T_e^0, \delta T_i/T_i^0, \delta V_i$) from the fixed field-aligned 42 m dish. The top panel is for 522 km and bottom panel for 450 km.

Figure 3 shows the time series of TID quantities ($\delta N_e/N_e^0, \delta T_e/T_e^0, \delta T_i/T_i^0, \delta V_i$) detected by the 42 m dish at two arbitrary altitudes in the ionospheric F-region. It is clearly seen that wavelike structures were also found in the fluctuations of electron temperature, ion temperature and ion velocity. In addition, the time variations of δV_i seem to be roughly in anti-phase with the time variations of $\delta N_e/N_e^0$, in agreement with a key property of AGW-induced TIDs outlined theoretically by Kirchengast (1997). We believe, therefore, that this behaviour, together with the observed wavefront inclination of the relative fluctuations in electron density (Fig. 2d), provides convincing evidence that AGWs were responsible for the observed TID.

2.1.2 EISCAT UHF radar

Figure 4 shows field-aligned electron density measurements from the EISCAT UHF radar at Tromsø in the same format as Fig. 2. The blank period from 06:00–10:10 UT is due to an unfortunate data gap. Periodic fluctuations are also clear in the interval of ∼10:10–14:00 UT at altitudes higher than ∼250 km in panels c and d and the period is once again about 120 min. Inclined wavefronts of the TID, similar to those in Fig. 2d, are evident in the bottom two panels of Fig. 4. The time series of TID quantities ($\delta N_e/N_e^0, \delta T_e/T_e^0, \delta T_i/T_i^0, \delta V_i$) displayed in Fig. 5 once again provide convincing evidence that the observed TID must be associated with an upward propagating AGW.

It seems, therefore, that the TIDs shown in Figs. 2 and 4 correspond to the ionospheric compressions and rarefactions as an AGW, which were seen sequentially by the two field-aligned radar beams as the AGW propagated equatorward from somewhere poleward of Svalbard. The periods of the

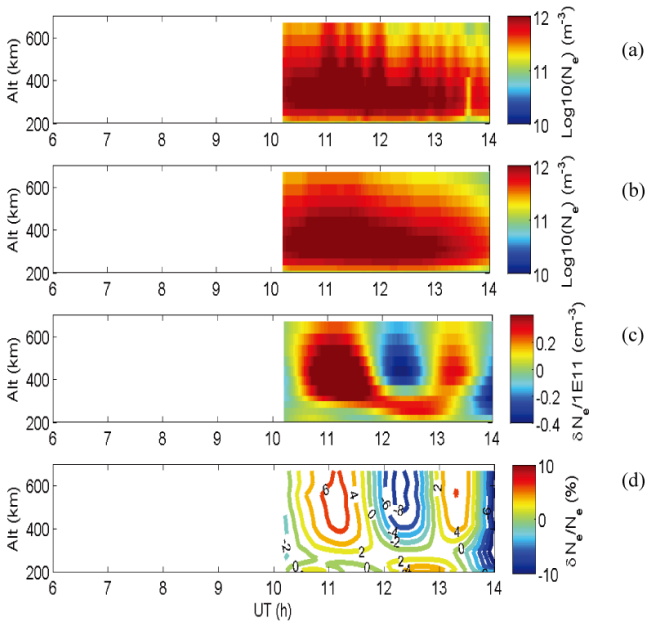

Fig. 4. The same as Fig. 2, but for the EISCAT UHF radar at Tromsø during the interval of 06:00–14:00 UT. The white space in the interval from 06:00 to 10:00 UT is due to a data gap.

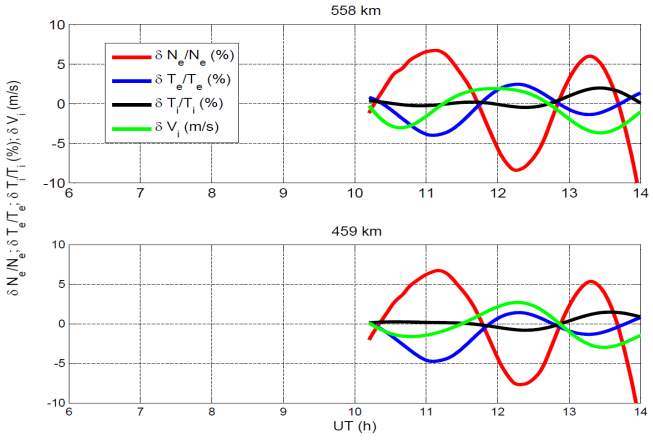

Fig. 5. The same as Fig. 3 but for the EISCAT UHF radar at 459 km (bottom panel) and 558 km (top panel). The white space in the interval from 06:00 to 10:00 UT is due to a data gap.

TIDs observed at Svalbard and Tromsø show a high degree of consistency, and in both radars the TID signatures are present over a wide vertical range from ∼230 km up to the topside of the ionospheric F-region with relatively little remarkable dissipation. One-to-one comparisons between Figs. 2d and 4d suggest an average time lag of ∼80 min between the AGW/TID observed at Svalbard and Tromsø. The positive (negative) perturbation around 11:10 UT (12:20 UT) at Tromsø (in Fig. 4d) seems to be the consequence of the ionization fluctuations detected around 10:00 UT (11:20 UT) by the ESR 42 m dish (in Fig. 2d) as the causative AGW moved equatorward. The density enhancement observed at Tromsø around 13:30 UT (in Fig. 4d) seems to correspond with the enhancement indicated at the rightmost edge of Fig. 2d. Electron density disturbances observed at Svalbard earlier than 09:00 UT are missed by the mainland UHF radar as it was not in operation until 10:10 UT.

From the time differences between the fluctuations in panel d of Figs. 2 and 4, we estimate the southward component of the AGW/TID phase speed to be ∼190 m s^{-1} (=8.3° latitudes per 80 min). A significant attenuation of the underlying wave can be inferred from the TIDs displayed in the two Figures, since the magnitude of the relative electron density fluctuations in the ionospheric F-region changed from ∼30 % at Svalbard to less than 10 % at Tromsø. This is probably because of AGW energy dissipation due to daytime ion drag, molecular viscosity and thermal conductivity during propagation.

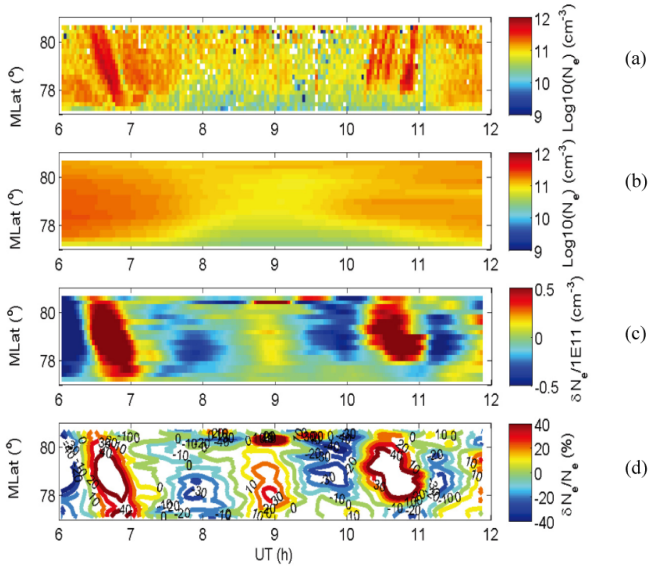

Fig. 6. The same as Fig. 2 but for the ESR 32 m dish, which was operating in low-elevation mode, directed toward the northern geomagnetic pole.

2.2 ESR observations in the polar cap

The electron density detected by the ESR 32 m dish on 13 February 2001, as a function of geomagnetic latitude and UT, is shown in Fig. 6a and the derived backgrounds (b), absolute (c) and relative (d) ionization fluctuations are also presented. During the plotted interval, the steerable 32 m dish was operating at low elevation (30°), covering a rather broad horizontal range in the polar cap up to ∼80° MLat. The spatial resolution along the radar beam was 36 km, leading to a horizontal resolution of 31 km and vertical resolution of 20 km.

Periodic positive/negative electron density perturbations are clearly presented in the bottom two panels of Fig. 6. These density perturbations were first detected at higher latitude (∼80° MLat) in the dayside of the northern polar cap, propagating gradually to lower latitudes. The period of the density disturbances is estimated to be ∼120 min, which is consistent with the disturbances observed by the field-aligned dishes at Svalbard and Tromsø, suggesting a clear linkage between the density fluctuations shown in the bottom panel of Figs. 2, 4 and 6.

Figure 6c and d show a significant positive perturbation in electron density around 07:00 UT. Panel a shows that this corresponds to an oblique structure of density enhancement, starting from 80° MLat and disappearing at ∼77.5° MLat. This electron density structure is accompanied by an equatorward motion, which subsequently reverses (not shown). These signatures are very similar to the characteristics of the Tongue of Ionization (TOI) which has been reported as being frequently observed near the dayside discontinuity region (e.g. Middleton et al., 2005 and references therein). In order to be certain that our analysis is only restricted to wave phenomena, this interval has been excluded from our subsequent dission, and only the remaining periodic density fluctuations (TIDs) in the interval 08:00–12:00 UT in Fig. 6 are focused on in the following sections, during which time the ESR radar saw no obvious signatures of TOI.

Periodic fluctuations in electron/ion temperature are less recognizable in the ESR 32 m radar data, probably due to the contaminating effect of electrodynamical processes in the dayside polar cap under conditions of moderately geomagnetic activity. Values of field-aligned δV_i are not available, since the ion velocity measured by the steerable 32 m dish is nearly perpendicular to the local geomagnetic field lines.

Even though TID signatures in other ionospheric parameters ($\delta T_e/T_e^0, \delta T_i/T_i^0, \delta V_i$) are absent, we suggest that the periodic electron density fluctuations detected by the low-elevation dish of ESR (Fig. 6d) can be interpreted as ionospheric oscillations due to a cross polar cap AGW propagating from the nightside to the dayside. As the AGW propagating sunward (equatorward) in the dayside polar cap, the induced TIDs were first recorded by the 32 m low-elevation dish at higher latitudes (∼80° MLat) and then at lower latitudes. After the AGW wavefront crossed the dayside boundary of the polar cap, the associated TID was consecutively measured by the field-aligned 42 m dish in the cusp and later by the UHF radar at Tromsø (under the dayside auroral oval) as it continued propagating southward.

Readers must keep in mind that, although the elevation of the 32 m dish was relatively low, the fluctuations shown in Fig. 6d must inevitably correspond to a mixture of horizontal and vertical variations in the plasma. Therefore, one must be careful in making interpretations of causative mechanisms for the observed electron density disturbances. In our case, however, the field-aligned observations at Svalbard and Tromsø summarized in Sect. 2.1 provide additional considerable supporting evidence for our hypothesis, strongly suggesting the presence of southward-propagating TIDs during this period.

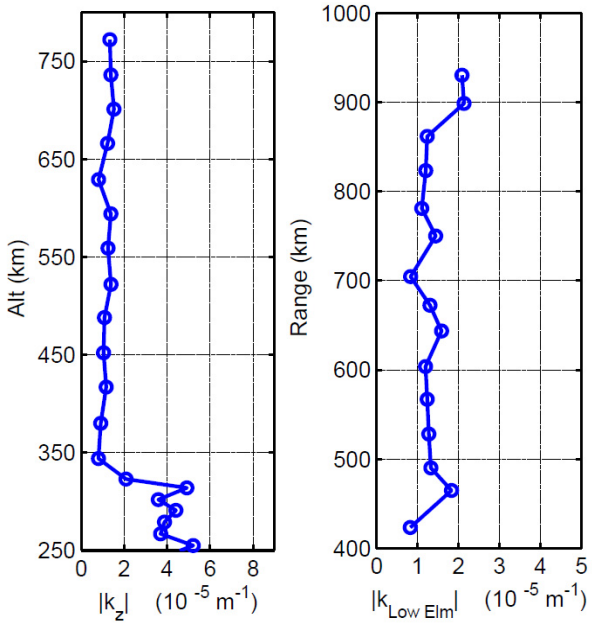

Fig. 7. Wave number components estimated along the two ESR radar beams using the method described by Ma et al. (1998), see text for details. The left-hand panel is for the field-aligned 42 m dish and the right-hand side panel is for the low-elevation 32 m dish.

3 Discussion

3.1 Properties of the polar cap AGW/TID

Components of wave number and phase velocity along the radar beam can be estimated by means of the phase differences between the signals at different altitudes (Ma et al., 1998). Figure 7 shows the wave number component, k_z, deduced from the field-aligned measurements of the ESR 42 m dish and the component along the look direction of the ESR 32 m dish, $k_{\mathrm{Low\_Elm}}$, respectively. Wave numbers shown in the figure were estimated by means of spectral analysis of time series of electron density fluctuations at various altitudes observed by the radar dishes during the whole period. It can be seen that the vertical component stayed approximately constant at altitudes above 350 km, implying that the polar cap AGW/TID maintained a rather stable inclination during the time interval of interest. The vertical wavelength is estimated to be ∼500 km. Cross-spectral analysis of field-aligned measurements yields a vertical phase speed of 62 m s^{-1}. The resulting vertical wave number is negative, implying downward propagation of the phase. Within the range window from 400 to 900 km along the low-elevation radar beam, the wave number $k_{\mathrm{Low\_Elm}}$ varied

slightly. Cross-spectral analysis of the measurements from the 32 m dish suggests a component of 158 m s^{-1} for phase speed towards the radar. Because of the low elevation of the 32 m dish, the wave number $k_{\mathrm{Low\_Elm}}$ can be used to make a rough estimate of the horizontal wavelength which is found to be ∼980 km. These propagation characteristics suggest a moderately large-scale polar cap AGW/TID. Assuming that the AGW/TID was in form of a monochromatic planar wave, its vector of phase speed in the meridional plane could be determined from the components measured in the two different directions (non-parallel). Calculations yielded a phase speed vector of 60 m s^{-1} with a sharply downward tilt (∼83°) in the meridional plane.

The electron density measurements from the 32 m dish used in the present work was integrated in two minutes. Assuming a typical horizontal phase speed of 200 m s^{-1} over the polar cap (MacDougall et al., 1997), the displacement of the AGW/TID within this integation period would be of order of 2 min × 200 m s^{-1} = 24 km, smaller than the spatial resolution of the radar (∼31 km). Therefore, provided that the horizontal speed of the AGW/TID is not extremely high, the observations of the 32 m dish would constitute an acceptable snapshot of the spatial distribution of the TIDs at a fixed time. With this assumption, we are able to examine the horizontal structure of the AGW/TID field in the dayside polar cap, using measurements from the low-elevation dish of the ESR.

Figure 8 showes a series of spatial snapshots of relative perturbations in electron density measured by the 32 m dish at five times around 10:30 UT. A positive density perturbation was first seen around 79.3° MLat at 10:11 UT (panel a) and then became evident (>20 %) around 10:24 UT (panel b) covering more than 200 km horizontally along the meridian. As time went by, the positive ionization enhancement moved gradually equatorward. Panel e shows the rarefactions observed after the passage of the ionization bulge.By comparing the peak-to-peak variations of the enhancement seen in Fig. 6d with those in the neighbouring panels, the meridional component of the horizontal phase speed for this southward-propagating ionization feature is roughly estimated to be 130 m s^{-1}. Calculations based on the comparison of the other panels in Fig. 6 exhibit similar characteristics.

We lack any azimuth information about the propagation of these polar cap AGW/TIDs due to the absence of any observations outside the plane defined by the two dishes of the ESR. Nevertheless, the sunward component (equatorward at the dayside) of the horizontal phase speed in the meridian can be inferred clearly by combining the observations from ESR (the 32 m and 42 m dishes) and the mainland UHF radar, which implies that the observed polar cap AGW/TID must be from somewhere on the nightside (Innis and Conde, 2002). One should remind that the strength of westward electrojects show a temporal increase (decrease of AL index) at 06:00 UT in Fig. 1, accompanied by a sudden enhancement of the Polar Cap Index derived from geomagnetic data obtained at Thule

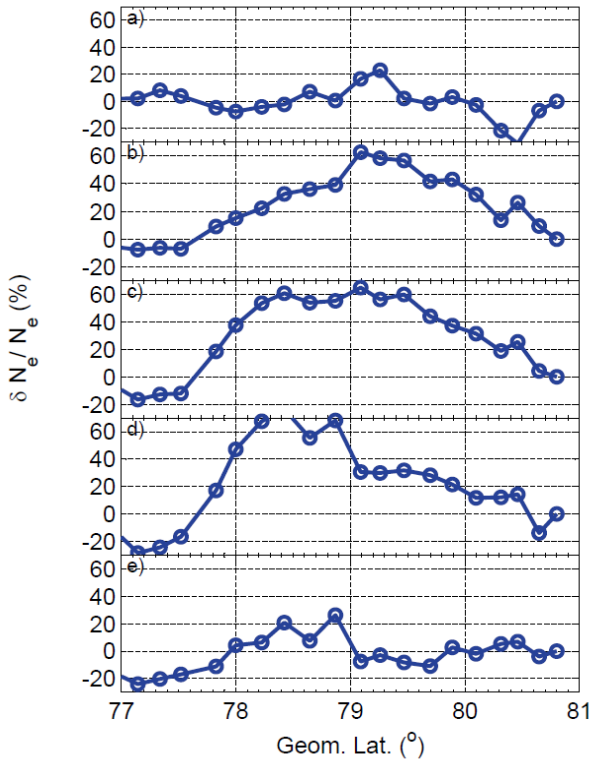

Fig. 8. Spatial variations of electron density perturbations measured by the ESR 32 m dish in dayside polar cap. From top to bottom, panels present relative electron density disturbances vs. geomagnetic latitude at selected intervals: **(a)** 10:11 UT; **(b)** 10:24 UT; **(c)** 10:31 UT; **(d)** 10:48 UT and **(e)** 1106 UT.

(∼02:00 LT). These signatures may be regarded as implying the existence of geomagnetic activity taking place somewhere on the nightside. There is strong evidence that high-latitude AGW sources are localized in or near the auroral oval (e.g. Sakanoi and Fukunishi, 1999; Oyama et al., 2001). Pervious statistical investigations also revealed that polar cap gravity waves frequently originate from sources in or near the midnight-dawn auroral oval (Innis and Conde, 2002) and that the horizontal phase progression is from the nightside to the dayside (Johnson et al., 1995). Therefore, we suggest that the polar cap AGW/TID observed here is likely to have been generated in the nightside auroral region during substorm conditions (Davis, 1971). The resulting wavess, propagating poleward across the polar cap from nightside to dayside, were detected by the ESR radar when Svalbard was in the right position.

3.2 Comparison with previous results

The propagation properties of the observed ionization waves suggest the presence of a moderately large-scale AGW/TID traveling across the northern polar cap. Generally, large-scale TIDs have been observed predominately at mid- and

low-latitude regions, which propagate from high latitudes (e.g. Shiokawa et al., 2007; Ding et al., 2008). Simultaneous observations of large-scale TIDs in both hemispheres are presented by Valladares et al. (2009), propagating from both auroral regions toward the geographic equator during the Halloween storm. The large-scale TID reported in the present paper distinguishes itself as having poleward propagation from night-time auroral source. Our results suggest that a poleward-propagating large-scale TID can cross the polar cap from the nightside to the dayside and then propagate equatorward, following which it would be expected to be observable in the dayside mid- and low-latitude regions.

In the polar cap, the observed AGW/TID in our case seems to be persistent with relatively little dissipation over a wide vertical range, from ∼230 km up to the topside of the ionospheric F-region. This is in agreement with the low attenuation of upward energy fluxes for polar cap gravity waves at altitudes from 250 to 560 km sampled by orbital passes of the DE-2 satellite (Johnson et al., 1995). A moderate level of energy dissipation for AGWs in the polar cap was also reported by Innis (2000).

In our case, the ESR radar detected significant relative ionization fluctuations (typical ∼20 % with some values >40 %) in the ionospheric F-region over the dayside polar cap, whilst Johnson et al. (1995) found little or no evidence of such plasma density oscillations from their in-situ observations of AGWs. On the other hand, MacDougall et al. (1997) found that significant raising of lowering of the ionosphere, and predicted that noticeable ionization fluctuations would exist near the bottom of the F-region, where density gradient with altitude is high. Our results provide direct observations of spatial distributions of ionization fluctuations at most altitudes over the polar cap, induced by AGW.

The magnitude of electron the relative fluctuation in electron density over the polar cap in our case is considerably larger than the typical fluctuations observed in the auroral oval (e.g. the cases reviewed by Hocke and Schlegel, 1996; Ma et al., 1998 and references therein), which is generally not higher than 10 %. On the other hand, TIDs induced by the cross polar cap AGW were detected at auroral latitudes in the altitude range from 300 up to 650 km (Fig. 4) with a magnitude of only 6–8 %. This could be explained by the dissipation of the wave during its horizontal propagation due to daytime ion drag, molecular viscosity and thermal conductivity. An alternative interpretation of the large ionization fluctuations observed over the polar cap would be attribute them to spatial resonance effects due to neutral wind speeds being comparable with the group speed of the observed TID (Kelley, 1989). One may also note that the background electron density in the polar cap (Fig. 6a) is much smaller than that in the auroral oval (Fig. 4a) whilst the absolute ionization fluctuations in the two regions (panel c of Figs. 4 and 6) are comparable with each other.

The horizontal phase speed of our observed polar cap AGW/TID is comparable with the typical values reported by MacDougall et al. (1997). The period in our case (around 120 min), however, is significant longer than what has previously been observed in the polar cap (Johnson et al., 1995; MacDougall et al., 1997). A noticeable discrepancy of wave periods, between observations from satellite and ground-based instruments over the cap, was also reported by MacDougall et al. (1997). Doppler shifting of the waves, as seen by a fixed observer was proposed by MacDougall et al. (1997) to give an acceptable explanation for the discrepancies. In our case, the ion bulk velocity along the line of sight from the 32 m dish indicated continuing anti-sunward (poleward) plasma convection during the interval of ∼08:00–11:00 UT (not shown). If we follow the idea that the resuting period of the AGW/TID has been systematically shifted to lower frequency due to anti-sunward plasma convection, the actual value of the wave period could be estimated. Average value of the ion velocity measured by the 32 m dish during the interval of ∼08:00–11:00 UT is around $450\,\mathrm{m\,s^{-1}}$. Assuming that the horizontal phase progression of the AGW/TID was anti-parallel to the ion bulk convection, the actual wave speed would have been $158–450\cos 180^\circ = 608\,\mathrm{m\,s^{-1}}$. Because of the low elevation of the 32 m dish, the phase speed component and the ion velocity along the radar beam are used here in order to make a rough estimation. Since this wave velocity is nearly four times larger then the directly calculated value of $158\,\mathrm{m\,s^{-1}}$, the period that would be measured on a fixed location if this wave would propagate in a stationary medium would be four times shorter, i.e. $120\,\mathrm{min}/4 = 30\,\mathrm{min}$, which is only slightly longer than the value of 850 s estimated from DE-2 observations by Johnson et al. (1995). On the other hand, even under magnetically quiet conditions with negligible plasma convection, southeastward directed AGW/TIDs with central period of 72 min have ever been observed in auroral region around magnetic local noon (Ma et al., 1998). We note that all of the gravity wave groups analyzed by MacDougall et al. (1997) were sampled on the nightside of the polar cap, whilst the AGW/TID in our case was detected on the dayside around magnetic local noon. Since the period might be lengthened due to spatial spreading effect of the wave packet (Francis, 1974), a lower frequency might be expected at the dayside if the source regions of AGW/TID were assumed to be located somewhere on the nightside. Thus, it seems that the combined effects of Doppler shifting and period lengthening may give a reasonable interpretation for the apparent discrepancy between our observations and those reported in previous studies.

Readers should also keep in mind that different source mechanisms could also affect the observed wave spectrum. Concerning the large-scale TIDs, the apparent period in our case should be a typical one, since large-scale TIDs with much longer period (∼3 h) have ever been observed as reviewed by Hunsucker (1982).

4 Summary

We have presented experimental evidence which indicates the trans-polar propagation of large-scale AGW/TIDs, which are generally accepted to be generated primarily in the nightside auroral region. The observed polar cap AGW/TID seems to have been launched on the nightside during substorm activity, and to have propagated poleward from the source region. The poleward-moving waves cross the polar cap from nightside to dayside and then are detected consecutively by the ESR (over the polar cap and then in the cusp) and by the mainland UHF radar (in the auroral oval) around geomagnetic local noon. Our results agree with the findings of theoretical simulations by Balthazor and Moffett (1999) in which poleward-propagating large-scale traveling atmospheric disturbances were self-consistently driven by enhancements in auroral heating.

Significant relative fluctuations in electron density are found in the ionospheric F-region at altitudes above ∼230 km over the polar cap, suggesting a wave phenomenon quite different to that predicted by MacDougall et al. (1997).

The quality of these observations also illustrates the merits of EISCAT/ESR facilities to investigate the ionosphere and thermosphere at extremely high latitudes.

Acknowledgements. We are grateful to the director and staff of the EISCAT Scientific Association for providing the radar facilities and assistance with making the observations. EISCAT is an international scientific association funded by the research councils of China, Finland, Germany, Japan, Norway, Sweden and the UK. This work was supported by Natural Sciences Foundation of China (No. 40874079) and Ocean Public Welfare Scientific Research Project, State Oceanic Administration People's Republic of China (No. 201005017).

Topical Editor K. Kauristie thanks three anonymous referees for their help in evaluating this paper.

References

Balthazor, R. L. and Moffett, R. J.: Morphology of large-scale traveling atmospheric disturbances in the polar thermosphere, J. Geophys. Res., 104, 15–24, 1999.

Davis, M. J.: On polar substorms as the source of large-scale traveling ionospheric disturbance, J. Geophys. Res., 76, 4525–4533, 1971.

Ding, F., Wan, W., Liu, L., Afraimovich, E. L., Voeykov, S. V., and Perevalova, N. P.: A statistical study of large-scale Traveling ionospheric disturbances observed by GPS TEC during major magnetic storms over the years 2003–2005, J. Geophys. Res., 113, A00A01, doi:10.1029/2008JA013037, 2008.

Francis, S. H.: A theory of medium-scale traveling ionospheric disturbances, J. Geophys. Res., 79, 5245–5260, 1974.

Hall, G. E., MacDougall, J. W., Cecile, J.-F., Moorcroft, D. R., and St.-Maurice, J. P.: Finding gravity wave source positions using the Super Dual Auroral Radar Network, J. Geophys. Res., 104, 67–78, 1999.

Hines, C. O.: Internal tmospheric gravity waves at ionospheric waves at ionospheric heights, Can. J. Phys., 38, 1441–1481, 1960.

Hocke, K.: Tidal variations in the high-latitude E- and F-region observed by EISCAT, Ann. Geophys., 14, 201–210, doi:10.1007/s00585-996-0201-9, 1996.

Hocke, K. and Schlegel, K.: A review of atmospheric gravity waves and travelling ionospheric disturbances: 1982–1995, Ann. Geophys., 14, 917–940, doi:10.1007/s00585-996-0917-6, 1996.

Hunsucker, R. D.: Atmospheric gravity waves generated in the high-latitude ionosphere: A review, Rev. Geophys., 20, 293–315, 1982.

Innis, J. L.: Deceleration of the high-latitude thermospheric wind by polar cap gravity waves, Geophys. Res. Lett., 27, 3813–3816, 2000.

Innis, J. L. and Conde, M.: High-latitude thermospheric vertical wind activity from Dynamics Explorer 2 Wind and Temperature Spectrometer observations: Indications of a source region for polar cap gravity waves, J. Geophys. Res., 107 pp., SIA 11-11, CiteID 1172, 2002.

Innis, J. L., Greet, P. A., and Dyson, P. L.: Evidence for thermospheric gravity waves in the southern polar cap from ground-based vertical velocity and photometric observations, Ann. Geophys., 19, 533–543, doi:10.5194/angeo-19-533-2001, 2001.

Johnson, F. S., Hanson, W. B., Hodges, R. R., Coley, W. R., Carignan, G. R., and Spencer, N. W.: Gravity Waves Near 300 km Over the Polar Caps, J. Geophys. Res., 100(A12), 23993–24002, 1995.

Kelley, M. C. (Ed.): The Earth's Ionosphere: Plasma physics and electrodynamics, Academic, San Diego, CA, 1989.

Kirchengast, G.: Elucidation of the physics of the gravity wave-TID relationship with the aid of theoretical simulations, J. Geophys. Res., 101, 13353–13368, 1996.

Kirchengast, G.: Characteristics of high-latitude TIDs from different causative mechanisms deduced by theoretical modeling, J. Geophys. Res., 102, 4597–4612, 1997.

Kirchengast, G., Hocke, K., and Schlegel, K.: The gravity wave-TID relationship: insight via theoretical model-EISCAT data comparison, J. Atmos. Sol.-Terr. Phy., 58, 233–243, 1996.

Ma, S. Y., Schlegel, K., and Xu, J. S.: Case studies of the propagation characteristics of auroral TIDS with EISCAT CP2 data using maximum entropy cross-spectral analysis, Ann. Geophys., 16, 161–167, doi:10.1007/s00585-998-0161-3, 1998.

MacDougall, J. W., Hall, G. E., and Hayashi, K.: F region gravity waves in the central polar cap, J. Geophys. Res., 102, 14513–14530, 1997.

Middleton, H. R., Pryse, S. E., Kersley, L., Bust, G. S., Fremouw, E. J., Secan, J. A., and Denig, W. F.: Evidence for the tongue of ionization under northward interplanetary magnetic field conditions, J. Geophys. Res., 110, A07301, doi:10.1029/2004JA010800, 2005.

Oyama, S., Ishii, M., Murayama, Y., Shinagawa, H., Burchert, S. C., Fujii, R., and Koffman, W.: Generation of atmospheric gravity waves associated with auroral activity in the polar F region, J. Geophys. Res., 106, 18543–18544, 2001.

Richmond, A. D.: Gravity wave generation, propagation and dissipation in the thermosphere, J. Geophys. Res., 83, 4131–4145, doi:10.1029/JA083iA09p04131, 1978.

Sakanoi, T. and Fukunishi, H.: Observations of vertical winds in

the thermosphere with a Fabry-Perot Doppler imager at Syowa station, Anntarctica, Adv. Space Res., 24, 1439–1422, 1999.

Shiokawa, K., Lu, G., Otsuka, Y., Ogawa, T., Yamamoto, M., Nishitani, N., and Sato, N.: Ground Observations and AMIE-TIEGCM modeling of a storm-time traveling ionospheric disturbance, J. Geophys. Res., 112, A05308, doi:10.1029/2006JA011772, 2007.

Valladares, C. E., Villalobos, J., Hei, M. A., Sheehan, R., Basu, Su., MacKenzie, E., Doherty, P. H., and Rios, V. H.: Simultaneous observation of traveling ionospheric disturbances in the Northern and Southern Hemispheres, Ann. Geophys., 27, 1501–1508, doi:10.5194/angeo-27-1501-2009, 2009.

Williams, P. J. S.: The generation and propagation of atmospheric gravity waves observed during the Worldwide Atmospheric Gravity-wave Study (WAGS), J. Atmos. Sol.-Terr. Phy., 50, 323–38, 1988.

Williams, P. J. S., Virdi, T. S., Lewis, R. V., Lester, M., Rodger, A. S., McCrea, I. W., and Freeman, K. S. C.: Worldwide atmospheric gravity-wave study in the European sector 1985–1990, J. Atmos. Sol.-Terr. Phy., 55, 683–696, 1993.

Yeh, K. C. and Liu, C. H.: Acoustic-gravity waves in the upper atmosphere, Rev. Geophys., 12, 193–216, 1974.